# Electronic structure and optical properties of ultrathin CdS/ZnS quantum wells grown by molecular-beam epitaxy

M. Hetterich, Ch. Märkle, A. Dinger, M. Grün, and C. Klingshirn
*Institut für Angewandte Physik der Universität Karlsruhe, Kaiserstraße 12, D-76128 Karlsruhe, Germany*
(Received 20 July 1998; revised manuscript received 2 November 1998)

We investigate in detail the optical properties of ultrathin, highly strained, cubic CdS/ZnS single and multiple quantum well structures using mainly photoluminescence, photoluminescence-excitation, and absorption spectroscopy. An effective model within the envelope function approximation is presented, taking into account strain and excitonic effects. Using an improved parameter set for cubic CdS this model successfully describes the observed exciton transition energies. A fit to experimental data taking into account the Stokes shift between luminescence and absorption yields some information about the model parameters, namely, the CdS/ZnS band alignment and the tetragonal deformation potential of CdS in the zinc-blende modification. Finally, we investigate the influence of localization effects due to well width fluctuations on the dimensionality of exciton confinement. A strong enhancement of the excitonic exchange interaction is found for deeply localized states in extremely narrow quantum wells, suggesting a significant lateral confinement and the formation of quasi-zero-dimensional states. [S0163-1829(99)08715-9]

## I. INTRODUCTION

Over the last few years, quantum structures based on the II-VI compounds CdS and ZnS have attracted continuous attention, because the wide and direct band gap of these materials could lead to potential applications for optoelectronic devices in the blue and UV spectral region. Accordingly, most publications up till now seem to focus either on the epitaxy and characterization of such structures[1–8] or on topics like nonlinear optical properties[9] and stimulated emission.[10–12] Further, due to the high lattice mismatch between CdS and ZnS, nearly exclusively superlattices—mostly containing the alloy (Cd,Zn)S—have been studied. Only a comparably small number of papers[6–8,12,13] deal with the properties of CdS/ZnS single and multiple quantum wells, and only little is known about the band alignment in this material system.[11,14–16]

In this paper, we discuss the optical properties of ultrathin cubic CdS/ZnS single quantum wells (SQWs). These structures have already been investigated recently by our group with an emphasis on structural aspects such as growth morphology, elastic and plastic strain relaxation.[17] As it turned out, no true strain-induced Stranski-Krastanow growth mode occurs during CdS quantum well deposition for the chosen experimental conditions, despite the high lattice mismatch of $-7\%$. Nevertheless the surface roughens more and more with increasing well thickness which should significantly influence the electronic properties of the investigated ultrathin quantum structures. Indeed, strong evidence for pronounced localization effects leading even to the formation of quasi-zero-dimensional states has been found, as discussed in Refs. 18–21 and below.

In this paper, we first review some of the optical properties of CdS/ZnS SQWs and then focus on the question of to what extent these properties can be described within the quantum well picture. Especially, an *effective* model applying the envelope function approximation is presented, taking strain and excitonic effects into account. From a fit to experimental data the model parameters, namely, the tetragonal deformation potential $b$ of CdS (see below) and the CdS/ZnS band alignment, are derived. The values obtained are compared to results of other authors and theoretical predictions. In a second step we investigate the effects of exciton localization on the optical properties of CdS/ZnS SQWs. Particularly, we discuss the influence on the excitonic exchange interaction from which—as shown below—information about the degree of lateral confinement in the quantum structures can be extracted.

## II. EXPERIMENTAL DETAILS

The investigated CdS/ZnS SQWs were grown by compound source molecular-beam epitaxy (MBE) on Si-doped GaAs(100) with no nominal miscut at a substrate temperature of 140 °C. They comprise relatively thin ZnS buffer and cap layers in most cases (typically about 100 nm and 50 nm, respectively) to prevent the appearance of disturbing Fabry-Pérot resonances in the spectra. The CdS quantum-well thicknesses of the different samples cover the whole range from the submonolayer region up to the critical value of 3 monolayers[17] (ML) for the onset of plastic strain relaxation. Further details about the growth process, thickness calibration, and structural aspects concerning the CdS/ZnS SQWs may be found in Ref. 17.

The photoluminescence (PL) measurements discussed below were recorded at $T=6$ K. For excitation we frequently used the 366-nm line extracted from the spectrum of a Hg lamp (200 W) by a prism double monochromator. In some cases (for the SQWs with the smallest well widths, i.e. the highest transition energies) the 313-nm line of the lamp or one of the UV lines of an $Ar^+$ laser had to be applied instead. The luminescence signal was dispersed by a 27.5-cm Czerny-Turner grating monochromator and detected by an optical multichannel analyzer. The same setup was also used for absorption measurements, where the continuous spectrum

 

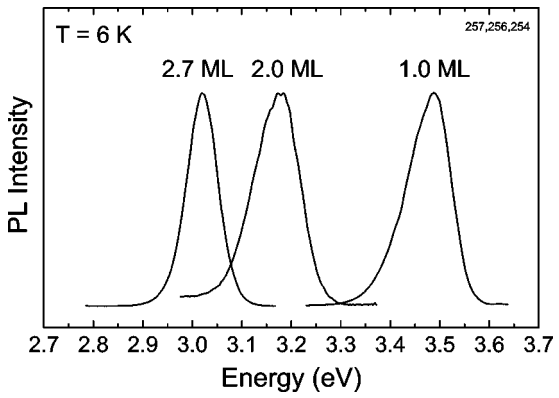


FIG. 1. Photoluminescence of three CdS/ZnS SQWs with different well width (1.0 ML, 2.0 ML, and 2.7 ML), excited below the ZnS band gap. The spectra were measured at $T=6$ K and are normalized to the PL maxima.

of a Xe lamp (500 W) served as the light source. To record photoluminescence-excitation (PLE) spectra, the desired excitation wavelength could be extracted from the emission of the latter by a 1-m grating monochromator. The detection in this case consisted of a 27.5-cm Czerny-Turner double monochromator and a GaAs photomultiplier utilizing a lock-in technique.

## III. RESULTS AND DISCUSSION

### A. PL, PLE, and absorption measurements

Figure 1 shows typical PL spectra for three CdS/ZnS SQWs with different well widths. A broad band assigned to the radiative recombination of localized excitons[18–21] is obtained in any case. The measured peak positions agree fairly well with those reported in Ref. 7. As expected, a shift to higher energies with decreasing well width due to the increasing quantization of charge carriers can be observed (see also inset of Fig. 5). The luminescence bands show a remarkable full width at half maximum (FWHM) of 80–110 meV (Fig. 2). As easily proved by resonant PL measurements, the corresponding broadening has an inhomogeneous nature, because tuning the excitation energy into the luminescence band induces a quenching of the emission above the excitation (see Fig. 6 discussed below). This inhomogeneous broadening is caused by thickness fluctuations of the ultrathin wells, leading to a spatial variation in exciton energy.

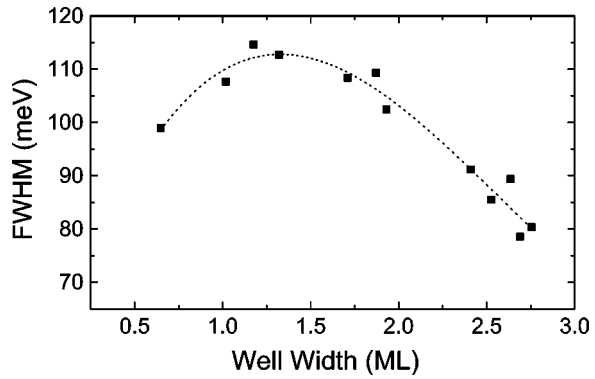


FIG. 2. Well width dependence of the PL full width at half maximum (FWHM). The dotted line is just to guide the eye.

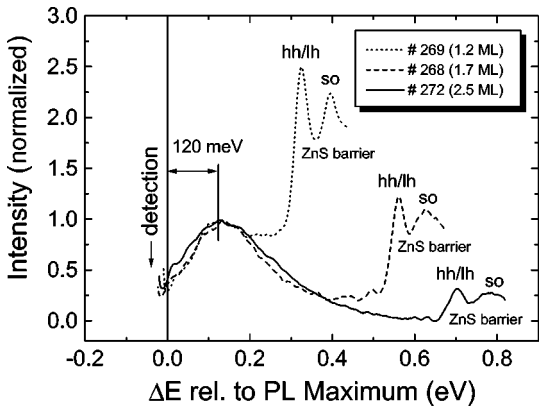


FIG. 3. PLE spectra of three SQW samples with different well widths, measured at $T=6$ K. Energies are given as shifts $\Delta E$ relative to the positions of the respective PL maxima. The spectra are normalized to their maximum at $\Delta E \approx 120$ meV.

Indeed, these lateral fluctuations could be directly visualized (of course averaged over the instrumental resolution) by spatially resolved near-field optical reflection spectroscopy of the SQWs.[22]

The observed behavior of the PL FWHM with well thickness shown in Fig. 2 is interpreted as follows: For very small widths the inhomogeneous broadening increases with increasing well thickness. One reason for this is the fact that the quantum well roughens more and more with proceeding CdS deposition, as discussed in Ref. 17. Additionally, the length scale of roughening will also increase with well thickness (many small nuclei are initially formed that spread when growth proceeds) so that the exciton can no longer ''average out'' the fluctuations. For thicker SQWs the absolute roughness approaches its equilibrium value. Therefore, the influence of lateral variations in well width on the exciton energy decreases with total SQW thickness, i.e., the inhomogeneous line broadening goes through a maximum and then drops with increasing well width.

Since the spatial fluctuations of the exciton energy can be regarded as a random lateral potential for the excitons, the density of states for the latter should be significantly modified and a low energy tail of localized states is expected to appear, which indeed expresses—apart from other effects discussed later on—in the asymmetric shape of the luminescence bands, especially for the thinner SQWs (see Fig. 1). In a quantitative analysis of PL data—as carried out below—one has to take into account that the predominant occupation of low energy tail states causes a Stokes shift of luminescence compared to, e.g., absorption so that the PL maximum does not exactly correspond to the average transition energy of the quantum well. To get some information about this Stokes shift we have measured PLE instead of absorption spectra because of the low optical thickness of the SQWs. The results for three samples with different well widths are shown in Fig. 3. Apart from peaks due to the heavy-hole/light-hole (hh/lh) and split-off exciton (SO) of the ZnS barrier a quantum well related broad band with similar shape in any case appears, the maximum of which is shifted by approximately 120 meV to higher energies with respect to the corresponding PL maximum. The interpretation of this structure is not obvious at first sight. Especially, the strong decrease of intensity observed in the PLE spectra for excitation

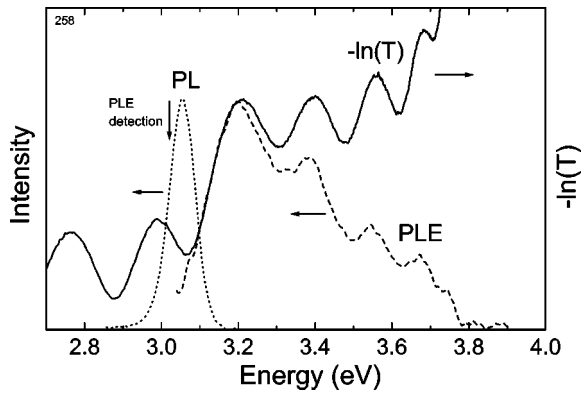


FIG. 4. Comparison of transmission $T$, photoluminescence (PL), and photoluminescence-excitation spectrum (PLE) of a 2.8-ML MQW sample at $T=6$ K.

energies far above the PL maximum is unexpected, because a steplike contribution caused by exciton continuum absorption should appear there. To clarify this point, some multiple quantum well structures (MQWs), each containing 20 identical wells separated by 30 nm ZnS spacers, were grown and the GaAs substrates have been etched away to enable optical transmission measurements. The result for a sample with a 2.8-ML well width is shown in Fig. 4, together with the corresponding PL and PLE spectra, respectively. Since the total thickness of the MQW structures is necessarily higher in comparison to SQW samples, the spectra are modulated by Fabry-Pérot resonances here. Nevertheless, the transmission clearly shows the expected steplike exciton continuum absorption. (The contribution above $\approx 3.7$ eV is caused by absorption in the ZnS buffer and barriers.) Therefore, the drop observed in PLE spectra for higher excitation energies does not reflect the energy dependence of the initial absorption, but is simply caused by a decrease in luminescence efficiency at the detection wavelength, when the energetic distance between excitation and detection is increased. The latter decrease of PL efficiency for nonresonant excitation results most likely from the fact that the created electron-hole pairs have to dissipate their surplus energy first, before they can recombine and emit a photon at the detection wavelength. During this relaxation process nonradiative recombination can take place, the possibility of which increases with the energetic distance to be bridged. [Of course there also exists the possibility of radiative (hot) recombination already above the detection window.]

Coming back to the question of Stokes shift between PL and absorption, it is important to note that the onset of quantum well absorption is in any case well reproduced in the PLE spectrum, as can be seen in Fig. 4. PLE therefore principally enables one to determine the Stokes shift also for the SQW samples, where no disturbing Fabry-Pérot modes appear but direct absorption measurements are impossible. The problem is, however, that neither absorption nor PLE spectra show any resolved peaklike features corresponding to bound (e.g., 1$s$) exciton states. Instead, the latter are merged with the continuum contributions due to the strong inhomogeneous broadening. For this reason, only a relatively crude estimation of the Stokes shift is possible by the use of curve fitting. Since only $n=1$ states can generally occur in our narrow quantum structures the spectra were fit by simply assuming a Gaussian-broadened discrete contribution to the density of states due to the e1-hh1 heavy-hole exciton transition and a correspondingly broadened steplike continuum contribution. The e1-lh1 light-hole exciton was not taken into account, because the absorption edge and the PL peak position should be determined by the energetically lower hh state. Additionally, the lh states have an intrinsically lower oscillator strength than the hh excitons which decreases even further due to the smaller overlap of their wave function with that of the electrons in comparison to the heavy holes. This is caused by the small valence band offset (see below) and the strain-induced hh/lh splitting leading approximately to flat band conditions for the light-hole states but a significant band offset for the hh.

Carrying out the fits as described one obtains values of about 60 meV for the energetic distance between the excitonic resonance in the tail of the absorption/PLE and the PL maximum. Hardly any dependence on well width is found (as already indicated by the nearly identical PLE spectra in Fig. 3), apart from the thickest wells, where the Stokes shift slightly decreases.

An interesting different approach to determine the Stokes shift directly from the FWHM of the PL can be extracted using a statistical topographical model for two-dimensional (2D) exciton luminescence discussed in Ref. 24. In this model, the excitons are assumed to be essentially trapped in the local minima of the lateral potential distribution (see above), leading to a nonthermal occupation of states. This assumption is not unreasonable in our case, because at the low measurement temperatures used, phonon-assisted hopping from one to another minimum is suppressed and tunneling through the maxima of the potential distribution is at least hampered, since localization is very strong in our system, leading to an ensemble of nearly decoupled states (see Refs. 18,19). Assuming the model described to be valid, we can combine the formulas given in Ref. 24 to obtain the simple relation

$$\Delta E_S = 0.6608 \times \Delta E_{\mathrm{PL}}, \tag{1}$$

where $\Delta E_S$ is the Stokes shift and $\Delta E_{\mathrm{PL}}$ is the FWHM of the luminescence band. A comparison of the $\Delta E_S$ values calculated using Eq. (1) with the results derived from transmission or PLE spectra showed surprisingly good agreement between both methods. For this reason, the Stokes shift was not always measured explicitly; in many cases it was much easier to extract it from the PL FWHM.

It is worth noting that assuming Eq. (1) to be true, Fig. 2 now explains why the Stokes shift between PL and PLE/absorption hardly depends on well width: Indeed, $\Delta E_S$ first increases slightly due to the increasing roughening of the quantum well before it decreases again as a result of the decreasing relative roughness of the well (see above). However, as can be seen in Fig. 2, the combination of both effects leads to a nearly constant Stokes shift. Only for the thickest wells should a significantly lower value be expected, in correspondence to the results obtained.

### B. Theoretical modeling of excitons and band alignment in CdS/ZnS SQWs

#### *1. Basic considerations*

In the following sections we investigate to what extent the experimental data presented above can be described within

TABLE I. Material parameters of unstrained cubic CdS and ZnS used in the calculations.

| Material parameter | Unit | CdS | ZnS |
|---|---|---|---|
| $E_g$ | (eV) | 2.48 [a] | 3.84 [b] |
| $a$ | (eV) | $-2.65$ [c, d] | |
| $b$ | (eV) | $\approx -0.5$ [e] | |
| $m_e$ | ($m_0$) | 0.2 [f] | 0.34 [g] |
| $m_{hh}$ | ($m_0$) | 1 [f, h] | 1.76 [i] |
| $a_0$ | (nm) | 0.5818 [g, c] | 0.54102 [g] |
| $c_{11}$ | (GPa) | 77.9 [j] | |
| $c_{12}$ | (GPa) | 52.7 [j] | |

[a]Reference 30.
[b]Reference 31.
[c]Reference 21.
[d]Reference 27.
[e]This work.
[f]Value for hexagonal material.
[g]Reference 32.
[h]Determined from exciton mass.
[i]Reference 34.
[j]Reference 33.

an idealized quantum well model. A fundamental problem here is that the CdS SQWs under discussion reveal thicknesses of only a few monolayers. The assumptions leading to the frequently applied envelope function approximation are therefore not *a priori* fulfilled within the well (see, however, the discussion below). Nevertheless we can adopt this approximation here at least as an *effective model* of our system with only a few adjustable parameters like the valence/conduction band offset. These parameters, once determined, may then easily be compared to results of other authors[11,14–16] using similar models or to theoretical expectations. Indeed, this procedure has also turned out to be of great practical advantage. For example, the *same* parameter set used for the SQWs discussed here can also be successfully applied to describe other quantum structures containing CdS/ZnS superlattices.[21,25]

A more practical problem in the quantitative modeling of CdS/ZnS SQWs is the fact that hardly any experimental data exist for cubic CdS. For this reason, CdS bulk layers have been grown and investigated by several methods to determine or confirm the required material parameters given in Table I as far as possible (for details see Ref. 21). The bulk values obtained are assumed to be approximately valid also for the ultrathin layers discussed here. This assumption seems to be reasonable within the achievable degree of accuracy when taking into account the effective character of the model and the fact that most material parameters are only crudely known anyway.

#### 2. Influence of strain on the CdS band structure

Due to the larger lattice constant of CdS in comparison to ZnS a compressive in-plane strain

$$\epsilon_{\parallel}=\epsilon_{xx}=\epsilon_{yy}=-7\% \tag{2}$$

occurs within the quantum well. The latter causes an additional distortion along the growth direction

$$\epsilon_{\perp}=\epsilon_{zz}=-2\frac{c_{12}}{c_{11}}, \tag{3}$$

where the $c_{ij}$ are the elastic moduli given in Table I. The strain-induced band shifts at $k=0$ can be calculated using the Hamiltonian of Pikus and Bir[26] which for tetragonal distortion ($\epsilon_{xy}=\epsilon_{yz}=\epsilon_{zx}=0$) reads

$$H_i^{\epsilon}=a_i(\epsilon_{xx}+\epsilon_{yy}+\epsilon_{zz})+3b_i[(L_x^2-\tfrac{1}{3}L^2)\epsilon_{xx}+\text{c.p.}]. \tag{4}$$

Here $i$ is the band index, $L$ the angular-momentum operator, $\epsilon_{ij}$ denotes the components of the strain tensor, and c.p. means cyclic permutation with respect to $x$,$y$ and $z$. The parameters $a_i$ and $b_i$ are the hydrostatic and tetragonal deformation potentials, respectively. Since we are primarily interested in the transition energy from the conduction band $c$ to the (heavy-hole) valence band $v$ it makes sense to look at the energy difference between the bands defining the relative deformation potentials

$$a:=a_c-a_v \quad \text{and} \quad b:=-b_v\,. \tag{5}$$

Notice that due to its $s$-like nature the conduction band edge is only affected by hydrostatic strain components. Combining Eqs. (2)–(5) leads to the strain Hamiltonian

$$H^{\epsilon}=2a\left(\frac{c_{11}-c_{12}}{c_{11}}\right)\epsilon_{\parallel}-3b\left(\frac{c_{11}+2c_{12}}{c_{11}}\right)\epsilon_{\parallel}\left(L_z^2-\frac{1}{3}L^2\right). \tag{6}$$

For the heavy-hole band ($|J,M_J\rangle=|3/2,3/2\rangle$) we simply have

$$\left(L_z^2-\frac{1}{3}L^2\right)\left|\frac{3}{2},\frac{3}{2}\right\rangle=\frac{1}{3}\left|\frac{3}{2},\frac{3}{2}\right\rangle. \tag{7}$$

The energetic shift of the conduction band relative to the heavy-hole valence band therefore is

$$\Delta E=2a\left(\frac{c_{11}-c_{12}}{c_{11}}\right)\epsilon_{\parallel}-b\left(\frac{c_{11}+2c_{12}}{c_{11}}\right)\epsilon_{\parallel}\,. \tag{8}$$

The hydrostatic deformation potential for cubic CdS has been experimentally determined by pressure-dependent optical absorption measurements of an epilayer with removed substrate in a diamond anvil cell to be $a=(-2.65\pm0.15)$ eV.[21,27] For $b$ only a single unusually high value ($b=-4.7$ eV) could be found in the literature.[28] We therefore decided to treat it as a fitting parameter here.

#### 3. Calculation of SQW transition energies

To calculate the quantum well transition energies a variational approach is used. We choose

$$\psi_{\lambda}(z_e,z_h,\rho)=\chi_e(z_e)\chi_h(z_h)\exp\left(-\frac{1}{\lambda}\sqrt{\rho^2+(z_e-z_h)^2}\right) \tag{9}$$

as the excitonic trial wave function and neglect the coupling between the different valence bands in our simplified model [an assumption which appears to be sufficient due to the strong strain-induced hh/lh splitting of $\approx 40$ meV and the very low quantization energy of the holes caused by the small valence band offset (see below)]. $\chi_e(z_e)$ and $\chi_h(z_h)$ in

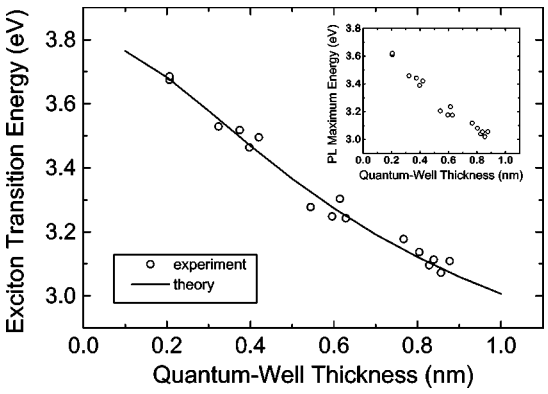


FIG. 5. Comparison of experimental exciton transition energies derived from PL measurements with model calculations assuming $b=-0.5$ eV and $\Delta V_{CB}=1.1$ eV. The original PL data are also given as an inset.

Eq. (9) are the well-known solutions of the finite square-well problem for the electrons and holes with effective masses $m_e$ and $m_h$ along the growth direction, respectively, demanding $\chi_{e,h}(z_{e,h})$ and $m_{e,h}^{-1}\partial\chi_{e,h}(z_{e,h})/\partial z_{e,h}$ to be continuous at the interfaces.[29] The third term in Eq. (9) takes into account the hydrogenlike nature of the system caused by the Coulomb interaction between electron and hole, where the variational parameter λ defines the exciton Bohr radius. Minimizing the energy expectation value for $\psi_\lambda(z_e,z_h,\rho)$ with respect to λ yields the desired exciton transition energy. (For further details, see Ref. 21.)

#### *4. Comparison with experiment*

In order to determine the adjustable parameters of our effective model, namely, the conduction band offset $\Delta V_{CB}$ and the tetragonal deformation potential $b$ of CdS, the exciton transition energy has been calculated as a function of well width and fitted to the experimental data (mainly taking into consideration the thickest quantum wells where the model should be most reasonable).

Figure 5 shows the result of this procedure, together with the experimental values derived from PL measurements and taking into account the Stokes shift as described above. (The original PL peak positions are also given in the inset of Fig. 5.) Excellent agreement between theory and experiment is achieved for a very reasonable parameter set which is discussed in detail below. Even for the thinnest SQWs one finds good correspondence, although the applied envelope function approximation (EFA) cannot *a priori* be expected to work properly in this region. This surprising result may possibly be related to the fact that for ultrathin SQWs the exciton wave function already penetrates strongly into the ZnS barrier (where the EFA is valid) and does not depend very much on details of the potential within the CdS well. The penetration of the wave function into the barrier also decreases the spatial variation of the envelope wave function and thus supports the validity of the EFA. Additionally, the valence band offset is very small (see below), so that the simplified treatment of the valence bands has no serious effect on the calculation of transition energies.

The parameters obtained from the fit in Fig. 5 are $b=-0.5$ eV for the tetragonal deformation potential of CdS and $\Delta V_{CB}=1.1$ eV for the strained conduction band offset. Comparing the value of $b$ with literature values for other II-VI materials [e.g., $b_{ZnS}=-0.53\ldots-0.7$ eV, $b_{ZnSe}=-1.2$ eV (Ref. 35)] suggests our result to be in a very reasonable range. When the absolute value of $b$ is increased substantially a satisfying fit cannot be achieved. Despite the simplified assumptions made in our model and some uncertainties in the other material parameters used this seems to indicate that the magnitude of the previously suggested value $b=-4.7$ eV for cubic CdS (Ref. 28) should be too high.

The second result of the fitting procedure described above, namely, $\Delta V_{CB}=(1.1\pm0.2)$ eV, means the occurrence of a type I band alignment in the quantum wells, where nearly the whole band gap difference between CdS and ZnS appears as a conduction band offset. Accordingly, there is only a small valence band discontinuity, which is in good agreement with the common anion rule. To enable a more detailed comparison with theory or results of other authors we have to remove the effects of strain-induced band shifts on the band alignment. This requires the hydrostatic deformation potentials for the individual CdS bands. Unfortunately the latter are not accurately known. Following the authors of Ref. 11 we therefore use $a_c\approx 2/3\ a$ which leads to an unstrained valence band offset of $\Delta V_{VB}^0=(180\pm200)$ meV. This result coincides very well with recent first-principle calculations suggesting exactly the same value as the ''natural'' offset for the CdS/ZnS system.[36] It is, however, somewhat lower than previously reported values derived only *indirectly* from the study of band offsets for different material combinations assuming transitivity [$\Delta V_{VB}^0\approx350$ meV (Ref. 14)] or from the investigation of $Cd_xZn_{1-x}S$/ZnS MQWs and superlattices combined with theoretical considerations [$\Delta V_{VB}^0\approx280$ meV (Refs. 11 and 16)], although there is still agreement within experimental error. Despite the effective nature of our model and the possible influence of different growth conditions on the band alignment via the atomic structure of the material interfaces the slight deviation of our value from previous results should most likely arise from the improved parameter set applied in our calculations and the fact that we take into account the effect of PL Stokes shift described above, which has formerly been neglected.

### C. Localization effects and lateral confinement

In the previous sections we have shown that the optical properties of ultrathin CdS/ZnS SQW structures can essentially be well described within an idealized quantum-well model. The occurrence of spatial well width fluctuations has only been discussed there as leading to an inhomogeneous line broadening and a Stokes shift between PL and absorption spectra. On the other hand, these fluctuations mean a laterally varying potential for the confined excitons, and the latter will therefore be localized in the minima of the resulting distribution (as already mentioned above). Typical localization depths should be in the same order of magnitude as the Stokes shift, i.e., about 60 meV. Similar results ($\approx$75 meV) are also obtained by fitting the temperature-dependent quenching of PL intensity using an Arrhenius-type model.[19] The values obtained not only clearly exceed thermal energies but are so high that at least for the most

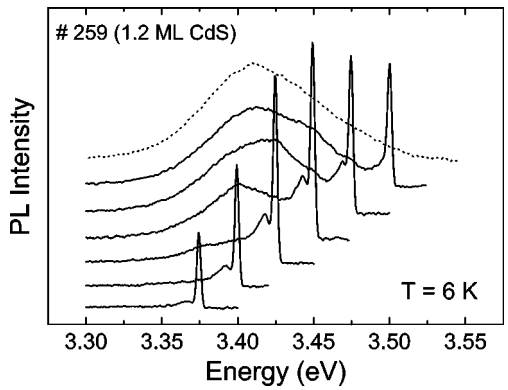


FIG. 6. Resonant PL spectra of a 1.2-ML quantum well for different excitation energies. For clarity the spectra are shifted relative to each other along the intensity axis.

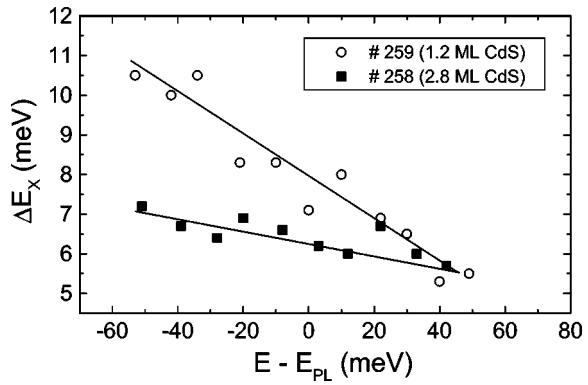


FIG. 7. Excitonic exchange splitting $\Delta E_x$ as a function of excitation (resonant PL) or detection (PLE) energy $E$ for quantum wells with 1.2 ML and 2.8 ML thickness, respectively. $E$ is given relative to the energetic position of the PL maximum $E_{\mathrm{PL}}$. The drawn lines are just to guide the eye.

deeply localized excitons tunneling during their lifetime from one potential minimum to another will be strongly hindered. These excitonic states can therefore be regarded as approximately decoupled. Such an interpretation is indeed supported by the results of time-dependent PL measurements and the observation of a broad ($\approx 200$ meV) spectral gain in high-excitation experiments (see Refs. 18–20 for details).

An interesting question arising in this context is to what extent the excitons are *laterally* confined through localization in the minima of the fluctuating potential, because a strong in-plane confinement should lead to the occurrence of quasi-zero-dimensional states. (It should, however, be noted that the correction of the corresponding confinement energies in comparison to the ideal quantum well model discussed above would not exceed the localization depth of about 60 meV which is negligible for the fit in Fig. 5, thus justifying the use of the idealized 2D model in the last section.) To clarify the influence of lateral confinement on the dimensionality of excitonic states, PL measurements under high spatial resolution have been carried out.[19,20] The obtained spectra show an ensemble of sharp luminescence peaks, indicating $\delta$-like contributions to the density of states. This observation suggests that quasi-zero-dimensional states could indeed exist in the investigated SQWs. To study this point in more detail, a different approach recently proposed[20] has been applied to get some further information about the degree of confinement, namely, the measurement of the excitonic exchange splitting. The latter scales with the probability of finding electron and hole at the same site and therefore strongly increases when the effective dimensionality is reduced from 3D towards a 2D quantum well.[37,38] An even stronger enhancement should be expected when a significant lateral confinement due to localization occurs additionally. To check this aspect, we have investigated the exchange splitting by PLE and resonant PL measurements. Results of the latter are shown in Fig. 6 for a sample with 1.2 ML well width and different excitation wavelengths. (For comparison, the ordinary PL is also shown as a dotted line.) Below the excitation a broad band caused by excitons having relaxed to deeper states can be observed in each case. The latter is slightly structured due to the coupling to phonons, which will not be discussed here in detail. No PL signal is detected above the excitation energy, indicating the luminescence to be *inhomogeneously* broadened. The dominant sharp peak in each spectrum corresponds to the recombination of resonantly excited localized excitons (with an additional small contribution of stray light from the excitation). Depending on the excitation energy used, a splitting of this peak (5–10 meV) into a double structure occurs. The latter can also be observed in PLE measurements and results from the excitonic exchange interaction, as proven mainly by polarization-dependent and time-resolved optical investigations.[20,23] For the dependence of the exchange splitting on the excitation energy two limiting situations may be distinguished: In ''*nearly ideal*'' SQWs well width fluctuations lead to exciton localization but lateral confinement is comparably weak. The recombination energy and exchange splitting of a localized exciton are therefore essentially determined by the local well thickness. Tuning the excitation to lower energies in this case means selecting quantum-well regions with wider well width, i.e., weaker confinement and therefore decreased exchange splitting. (It should, however, be noted that for the ultrathin SQWs investigated here the wave function already penetrates significantly into the barrier so that the confinement along the growth direction does not increase very much with decreasing well width.) The opposite holds for the other limit, where localization due to well width fluctuations becomes so dominant that a significant lateral confinement occurs which governs the exchange splitting (''*quasi-0D limit*''). In this case lowering the excitation energy corresponds to the selection of deeper localized states. Since lateral confinement should generally be enhanced with localization depth, an increasing exchange splitting with decreasing excitation energy should be observed here.

The experimentally obtained splitting $\Delta E_x$ as a function of excitation (resonant PL) or detection energy (PLE) $E$ is shown in Fig. 7 for two samples with 1.2 and 2.8 ML well width, corresponding to the cases of maximum and minimum localization strength [according to Fig. 2 and Eq. (1)]. An increase of the splitting occurs when tuning $E$ to lower energies. While this trend is only weak (or even reverses in some cases) for wider quantum wells, a strong increase of $\Delta E_x$ with decreasing $E$ is found when going to samples with very thin wells. In terms of the models discussed above this leads to the plausible result that with decreasing well width the electronic structure leaves the ''nearly ideal quantum-

well'' case more and more and approaches the ''quasi-0D'' limit, where localization induced by well width fluctuations plays a dominant role and causes a significant lateral confinement.

## IV. CONCLUSIONS

We have investigated ultrathin CdS/ZnS single and multiple quantum-well structures grown by MBE in detail using mainly PL, PLE, and absorption spectroscopy. The observed luminescence bands show a strong inhomogeneous broadening caused by thickness fluctuations of the wells. An effective theoretical model within the envelope function approximation has been successfully applied to describe the well width dependence of the PL peak energies, using an improved parameter set for cubic CdS. The model takes into account strain as well as excitonic effects and the Stokes shift between PL and absorption/PLE. A fit to the experimental data yields the model parameters, namely, the tetragonal deformation potential of CdS $b \approx -0.5$ eV and a CdS/ZnS unstrained type I valence band offset of $\Delta V_{VB}^{0} = (180 \pm 200)$ meV, which agrees very well with theoretical predictions for the ''natural'' offset.

In the second part of the paper we have discussed the influence of localization effects due to well width fluctuations on the dimensionality of exciton confinement. Especially, the excitonic exchange interaction could be shown to increase strongly for deeply localized states and extremely thin quantum wells. This result suggests that with decreasing well width the electronic structure leaves the ''nearly ideal quantum-well'' case more and more and approaches the ''quasi-0D'' limit, where localization induced by well width fluctuations plays a dominant role and causes a significant lateral confinement.

## ACKNOWLEDGMENTS

Professor Dr. U. Woggon and F. Gindele (University of Dortmund, Germany) are acknowledged for useful discussions concerning the excitonic exchange interaction. We also wish to thank Professor Dr. W. Gebhardt and E. Griebl (University of Regensburg, Germany) for pressure-dependent optical absorption measurements of a cubic CdS epilayer grown in our group. Finally, the Deutsche Forschungsgemeinschaft (DFG) is acknowledged for financial support.

[1] H. Fujiyasu, T. Sasaya, M. Katayama, K. Ishino, A. Ishida, H. Kuwabara, Y. Nakanishi, and G. Shimaoka, Appl. Surf. Sci. **33/34**, 854 (1988).
[2] S. Ohta, S. Kobayashi, F. Kaneko, and K. Kashiro, J. Cryst. Growth **106**, 166 (1990).
[3] P.J. Parbrook, P.J. Wright, B. Cockayne, A.G. Cullis, B. Henderson, and K.P. O'Donnell, J. Cryst. Growth **106**, 503 (1990).
[4] P.D. Brown, Y.Y. Loginov, K. Durose, J.T. Mullins, T. Taguchi, T. Burbery, S. Lawson-Jack, and I. Jones, J. Cryst. Growth **117**, 536 (1992).
[5] T. Tadokoro, S. Ohta, T. Ishiguro, Y. Ichinose, S. Kobayashi, and N. Yamamoto, J. Cryst. Growth **130**, 21 (1993).
[6] R.P. Vaudo, D.B. Eason, K.A. Bowers, K.J. Gossett, J.W. Cook, Jr., and J.F. Schetzina, J. Vac. Sci. Technol. B **11**, 875 (1993).
[7] G. Brunthaler, M. Lang, A. Forstner, C. Giftge, D. Schikora, S. Ferreira, H. Sitter, and K. Lischka, J. Cryst. Growth **138**, 559 (1994).
[8] C. Meyne, U.W. Pohl, J.-T. Zettler, and W. Richter, J. Cryst. Growth **184/185**, 264 (1998).
[9] J.T. Mullins and T. Taguchi, J. Cryst. Growth **117**, 501 (1992).
[10] Y. Yamada, Y. Masumoto, J.T. Mullins, and T. Taguchi, Appl. Phys. Lett. **61**, 2190 (1992).
[11] T. Taguchi, C. Onodera, Y. Yamada, and Y. Masumoto, Jpn. J. Appl. Phys., Part 2 **32**, L1308 (1993).
[12] K.B. Ozanyan, J.E. Nicholls, L. May, J.H.C. Hogg, W.E. Hagston, B. Lunn, and D.E. Ashenford, Solid State Commun. **99**, 407 (1996).
[13] H. Dumont, Y. Kawakami, Shizuo Fujita, and Shigeo Fujita, Jpn. J. Appl. Phys., Part 2 **34**, L1336 (1995).
[14] K.P. O'Donnell and B. Henderson, J. Lumin. **52**, 133 (1992).
[15] T. Taguchi, T. Ohno, and Y. Nozue, Surf. Sci. **267**, 141 (1992).
[16] T. Yokogawa, T. Ishikawa, J.L. Merz, and T. Taguchi, J. Appl. Phys. **75**, 2189 (1994).
[17] M. Hetterich, M. Grün, W. Petri, C. Märkle, C. Klingshirn, A. Wurl, U. Fischer, A. Rosenauer, and D. Gerthsen, Phys. Rev. B **56**, 12369 (1997).
[18] U. Woggon, W. Petri, A. Dinger, S. Petillon, M. Hetterich, M. Grün, K.P. O'Donnell, H. Kalt, and C. Klingshirn, Phys. Rev. B **55**, 1364 (1997).
[19] W. Petri, M. Hetterich, U. Woggon, C. Märkle, A. Dinger, M. Grün, C. Klingshirn, T. Kümmell, G. Bacher, and A. Forchel, J. Cryst. Growth **184/185**, 320 (1998).
[20] U. Woggon, F. Gindele, W. Petri, M. Hetterich, M. Grün, C. Klingshirn, W. Langbein, J.M. Hvam, T. Kümmell, G. Bacher, and A. Forchel, Phys. Status Solidi B **206**, 501 (1998).
[21] M. Hetterich, Ph.D. thesis, Universität Karlsruhe, Germany, 1998.
[22] W. Langbein, J.M. Hvam, S. Madsen, M. Hetterich, and C. Klingshirn, Phys. Status Solidi A **164**, 541 (1997).
[23] U. Woggon, F. Gindele, W. Langbein, and M. Hetterich, Phys. Status Solidi A **164**, 505 (1997).
[24] M. Wilkinson, F. Yang, E.J. Austin, and K.P. O'Donnell, J. Phys.: Condens. Matter **4**, 8863 (1992).
[25] M. Hetterich (unpublished).
[26] G.E. Pikus and G.L. Bir, Fiz. Tverd. Tela (Leningrad) **1**, 1642 (1959) [Sov. Phys. Solid State **1**, 1502 (1959)].
[27] M. Grün, M. Hetterich, C. Klingshirn, E. Griebl, and W. Gebhardt (unpublished).
[28] D.W. Niles and H. Höchst, Phys. Rev. B **44**, 10965 (1991).
[29] See, for example, G. Bastard, *Wave Mechanics Applied to Semiconductor Heterostructures* (Les éditions de physique, Paris, 1992).
[30] D.R.T. Zahn, G. Knudlek, U. Rossow, A. Hoffmann, I. Broser, and W. Richter, Adv. Mater. Opt. Electron. **3**, 11 (1994).
[31] M. Fernández, P. Prete, N. Lovergine, A.M. Mancini, R. Cingolani, L. Vasanelli, and M.R. Perrone, Phys. Rev. B **55**, 7660 (1997).
[32] *Landolt-Börnstein, Numerical Data and Functional Relationships*

*in Science and Technology, New Series*, edited by O. Madelung (Springer, Berlin, 1982), Group III, Vol. 17, Part 6.

[33] *Landolt-Börnstein, Numerical Data and Functional Relationships in Science and Technology, New Series*, edited by K.-H. Hellwege and A.M. Hellwege (Springer, Berlin, 1979), Group III, Vol. II.

[34] *Landolt-Börnstein, Numerical Data and Functional Relationships in Science and Technology, New Series*, edited by O. Madelung (Springer, Berlin, 1982), Group III, Vol. 22, Part a.

[35] A. Blacha, H. Presting, and M. Cardona, Phys. Status Solidi B **126**, 11 (1984).

[36] S.-H. Wei and A. Zunger, Appl. Phys. Lett. **72**, 2011 (1998).

[37] Y. Chen, B. Gil, P. Lefebvre, and H. Mathieu, Phys. Rev. B **37**, 6429 (1988).

[38] J. Puls, F. Henneberger, M. Rabe, and A. Siarkos, J. Cryst. Growth **184/185**, 787 (1998) and references therein.